DALTON
FULL PAPER

Synthesis and reactivity of triosmium nitrite clusters containing some functionalised amine ligands

Bernard Kwok-Man Hui and Wing-Tak Wong *

Department of Chemistry, The University of Hong Kong, Pokfulam Road, Hong Kong, P. R. China. E-mail: wtwong@hkucc.hku.hk

Received 7th July 1998, Accepted 16th October 1998

Reaction of $[Os_3(\mu\text{-H})(CO)_{10}(\mu\text{-}\eta^2\text{-}NO_2)]$ **1** with ammonia and some amines [2-phenylethylamine, octadecylamine, 4-*tert*-butylcyclohexylamine, piperidine-1-ethanamine (pipea) and 1-ethynylcyclohexylamine (echa)] afforded a pair of isomers **a** and **b** with general formula $[Os_3(\mu\text{-H})(CO)_9(\mu\text{-}\eta^2\text{-}NO_2)(NH_2R)]$, R = H **2a** and **2b**, CH_2CH_2Ph **3a** and **3b**, $(CH_2)_{17}CH_3$ **5a** and **5b**, $(C_6H_{10})Bu^t$-4 **6a** and **6b**, pipea **7a** and **7b** or echa **10a** and **10b**. Carbonylation of isomers **3a** and **3b** afforded $[Os_3(\mu\text{-H})(CO)_{10}(\mu\text{-NHCH}_2CH_2Ph)]$ **4**. Thermolysis of **7a** and **7b** afforded $[Os_3(\mu\text{-H})(CO)_{10}(\mu\text{-pipea} - H)]$ **8** and $[Os_3(\mu\text{-H})(CO)_9(\mu\text{-}\eta^2\text{-pipea} - H)]$ **9**. Thermolysis of **10a** resulted in hydride migration, from the metal core to the unsaturated carbons in the organic moiety, to give $[Os_3(CO)_9(\mu\text{-}\eta^2\text{-}NO_2)(\text{echa} + H)]$ **11**. All these clusters were fully characterised by solution spectroscopic methods and the solid state structures of **2a**, **4**, **5a**, **7b**, **8**, **9** and **11** were determined by X-ray crystallography.

Introduction

The activation of N–H bonds in triosmium and triruthenium clusters containing aliphatic or aromatic nitrogen ligands has been extensively investigated.[1–12] However, similar studies of triosmium nitrite clusters have been relatively unexplored. We have reported the synthesis of $[Os_3(\mu\text{-H})(CO)_{10}(\mu\text{-}\eta^2\text{-}NO_2)]$ **1** and its reactions with functionalised phosphines.[13,14] Further studies of the synthesis and properties of nitrite complexes are important and useful in understanding the chemistry of the NO_2^- moiety on metal cluster surfaces.

Studies of the stereochemistry of nickel(II) nitrite complexes with heterocyclic amines suggested that the co-ordination mode of the nitrite ligands should be strongly influenced by ligand–ligand steric interactions.[15,16] In order to extend the investigation, the reactivity of cluster **1** towards some selected amines with different steric factors and molecular shapes has been studied. A bidentate amine and an amine containing an unsaturated hydrocarbon side chain were also included so as to examine the possible reactivities of metal-bound NO_2 towards unsaturated hydrocarbons or intramolecular ligand displacement. It is believed that the reactions of this nitrite cluster with functionalised amines will also be useful to investigate the hydrogen migration and rearrangements of the nitrite ligand which may give us some insight towards understanding the chemistry of nitrite clusters.

Results and discussion

Reaction of $[Os_3(\mu\text{-H})(CO)_{10}(\mu\text{-}\eta^2\text{-}NO_2)]$ 1 with NH_3

Treatment of cluster **1** with an excess of 2.0 M ammonia solution (in propan-2-ol) in CH_2Cl_2 for 2 h afforded two orange products. The major product was characterised as $[Os_3(\mu\text{-H})(CO)_9(\mu\text{-}\eta^2\text{-}NO_2)(NH_3)]$ **2a**. The minor product is an isomer of **2a** namely cluster **2b**. The positive FAB mass spectra of clusters **2a** and **2b** show identical molecular ion peaks and hence suggest that they are isomeric but differ in the disposition of the NH_3 ligand towards the metal core. The ^1H NMR spectra of **2a** and **2b** display a single hydride resonance at δ −11.3 and −10.9 respectively. In the solution IR spectra both isomers show terminal co-ordinated carbonyl activities only, while the solid-state IR spectra (KBr disc) display the $\nu(NO_2)$ stretching frequencies at 1466 and 1136 and 1465 and 1135 cm^{-1}, respectively (Table 1).

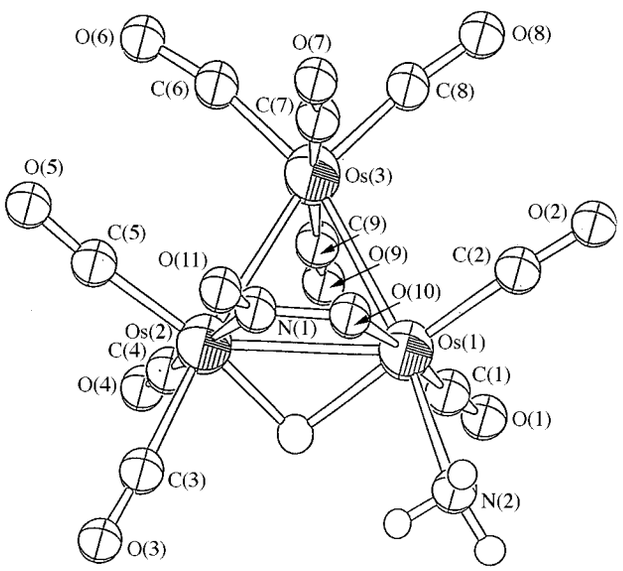

Fig. 1 Molecular structure of $[Os_3(\mu\text{-H})(CO)_9(\mu\text{-}\eta^2\text{-}NO_2)(NH_3)]$ **2a**.

Single crystals of cluster **2b** could not be obtained. Crystals of **2a** suitable for X-ray analysis were obtained by slow evaporation from a *n*-hexane solution. A perspective view of **2a** is given in Fig. 1, and selected bond parameters are in Table 2. Both isomers are not stable in solution, decomposing to brown insoluble solids which could not be further characterised.

Complex **2a** consists of an irregular triangular metal framework [Os(1)–Os(3) 2.822(2), Os(2)–Os(3) 2.853(2), Os(1)–Os(2) 2.908(2) Å]. The hydride and nitrite ligand bridge across the longest, Os(1)–Os(2), edge. The NH_3 moiety is terminally co-ordinated [Os(1)–N(2) 2.20(3) Å]. The nitrite ligand is bonded to the metal core *via* N(1) and O(10) [Os(2)–N(1) 2.04(2) and Os(1)–O(10) 2.14(2) Å]. The dihedral angle defined by the planes involving Os(1)–Os(2)–Os(3) and the NO_2^- moiety is 101.8°.

Cluster **2a** is believed to be slightly favourable to **2b** based on steric considerations, and this is supported by the observation of a higher yield of **2a** (35%) than that of **2b** (20%). Since the NO_2^- ligand is asymmetrically bonded to the metal core, it leads to differences in steric repulsion between the outstretched

Table 1 Spectroscopic data of compounds **2a**–**11**

Compound	IR/cm^{-1}	^{1}H NMR, δ (J/Hz)[a]	MS,[b] m/z
2a	ν(CO):[c] 2103m, 2060s, 2024vs, 1966m, 1939w ν(NO_2), KBr: 1466m, 1136w	3.0 [*s*, 3 H, NH_3], −11.3 [*s*, 1 H, Os–H]	887 (887)
2b	ν(CO):[c] 2104m, 2064s, 2022vs, 2007s, 1982w, 1951w ν(NO_2), KBr: 1465m, 1135w	3.2 [*s*, 3 H, NH_3], −10.9 [*s*, 1 H, Os–H]	887 (887)
3a	ν(CO):[c] 2104m, 2064s, 2022vs, 2007s, 1982w, 1951w ν(NO_2), KBr: 1484m, 1127w	7.4–7.2 [*m*, 5 H, Ph], 3.5 [*t*, 2 H, J_{HH} 6.9, NH], 1.4 [*br m*, 4 H, CH_2], −11.4 [*s*, 1 H, Os–H]	991 (991)
3b	ν(CO):[c] 2104m, 2068s, 2026vs, 2010s, 1979w, 1935w ν(NO_2), KBr: 1480m, 1130w	7.4–7.2 [*m*, 5 H, Ph], 3.8 [*t*, 2 H, J_{HH} 6.9, NH], 1.3 [*br m*, 4 H, CH_2], −11.5 [*s*, 1 H, Os–H]	991 (991)
4	ν(CO):[c] 2105w, 2064vs, 2051s, 2016s, 2003m, 1989m	7.3–7.2 [*m*, 5 H, Ph], 3.9 [*s*, 1 H, NH], 3.1 [*t*, 2 H, J_{HH} 6.6, CH_2], 2.8 [*t*, 2 H, J_{HH} 6.6, CH_2], −14.8 [*s*, 1 H, Os–H]	974 (972)
5a	ν(CO):[c] 2080s, 2018s, 2010s, 1968m, 1943m ν(NO_2), KBr: 1462m, 1150w	1.5–1.4 [*m*, 2 H, CH_2], 1.4–1.1 [*m*, 32 H, CH_2], 0.9 [*t*, 3 H, J_{HH} 7.1, CH_3], −11.3 [*s*, 1 H, Os–H]	1140 (1139)
5b	ν(CO):[c] 2104m, 2063s, 2023vs, 2006s, 1981w, 1952w ν(NO_2), KBr: 1461m, 1146w	1.4–1.3 [*s*, 2 H, CH_2], 1.3–1.1 [*m*, 32 H, CH_2], 0.9 [*t*, 3 H, J_{HH} 7.1, CH_3], −11.1 [*s*, 1 H, Os–H]	1139 (1139)
6a	ν(CO):[c] 2105w, 2068s, 2028vs, 2008s, 1998w, 1933w ν(NO_2), KBr: 1470m, 1126w	5.3 [*s*, 2 H, NH], 1.7–1.5 [*m*, 1 H, CH], 1.4–1.2 [*m*, 8 H, CH_2], 1.2–0.92 [*m*, 1 H, CH], 0.8 [*s*, 9 H, CH_3], −11.4 [*s*, 1 H, Os–H]	1024 (1025)
6b	ν(CO):[c] 2103m, 2064s, 2022vs, 2005s, 1982w, 1952w ν(NO_2), KBr: 1460m, 1143w	5.5 [*s*, 2 H, NH], 1.7–1.5 [*m*, 1 H, CH], 1.5–1.3 [*m*, 8 H, CH_2], 1.1–1.0 [*m*, 1 H, CH], 0.9 [*s*, 9 H, CH_3], −12.6 [*s*, 1 H, Os–H]	1024 (1025)
7a	ν(CO):[c] 2099m, 2066m, 2020vs, 2002s, 1968s, 1954m, 1943w ν(NO_2), KBr: 1460m, 1158w	5.3 [*t*, 2 H, J_{HH} 8.2, NH], 2.6–2.4 [*m*, 10 H, CH_2], 0.9–0.7 [*m*, 4 H, CH_2], −18.0 [*s*, 1 H, Os–H]	999 (998)
7b	ν(CO):[c] 2102m, 2063s, 2020vs, 2007s, 1981w, 1953w ν(NO_2), KBr: 1466m, 1145w	5.3 [*t*, 2 H, J_{HH} 7.8, NH], 2.5–2.3 [*m*, 10 H, CH_2], 0.9–0.8 [*m*, 4 H, CH_2], −16.2 [*s*, 1 H, Os–H]	999 (998)
8	ν(CO):[c] 2103w, 2062vs, 2049s, 2012s, 2005m, 1987m	4.2 [*s*, 1 H, NH], 2.8–2.5 [*m*, 10 H, CH_2], 1.0–0.8 [*m*, 4 H, CH_2], −14.9 [*s*, 1 H, Os–H]	980 (979)
9	ν(CO):[c] 2088m, 2045vs, 2005s, 1991s, 1983vs, 1967s, 1940w	4.3 [*s*, 1 H, NH], 2.6–2.4 [*m*, 10 H, CH_2], 0.9–0.8 [*m*, 4 H, CH_2], −13.5 [*s*, 1 H, Os–H]	951 (951)
10a	ν(CO):[c] 2106w, 2074m, 2005vs, 1995s, 1956w, 1933w ν(NO_2), KBr: 1463m, 1129w	5.6 [*s*, 2 H, NH], 5.2 [*s*, 1 H, CH], 0.9–0.8 [*m*, 10 H, CH_2], −11.2 [*s*, 1 H, Os–H]	994 (993)
10b	ν(CO):[c] 2103m, 2063s, 2022vs, 2007s, 1983w, 1951w ν(NO_2), KBr: 1460m, 1127w	5.3 [*s*, 2 H, NH], 4.2 [*s*, 1 H, CH], 0.9–0.8 [*m*, 10 H, CH_2], −10.9 [*s*, 1 H, Os–H]	994 (993)
11	ν(CO):[c] 2120w, 2099m, 2057s, 2024vs, 2008s, 1970w ν(NO_2), KBr: 1487m, 1131w	5.9 [*s*, 2 H, NH], 5.4 [*s*, 2 H, olefinic CH_2], 0.9–0.8 [*m*, 10 H, CH_2]	994 (993)

[a] Recorded in $CDCl_3$. [b] Calculated value in parentheses. [c] Recorded in CH_2Cl_2.

Table 2 Selected bond parameters (distances in Å, angles in °) of $[Os_3(\mu\text{-H})(CO)_9(\mu\text{-}\eta^2\text{-}NO_2)(NH_3)]$ **2a**

Os(1)–Os(2)	2.908(2)	Os(1)–Os(3)	2.822(2)
Os(2)–Os(3)	2.853(2)	Os(1)–N(2)	2.20(3)
Os(1)–O(10)	2.14(2)	Os(2)–N(1)	2.04(2)
O(10)–N(1)	1.36(3)	O(11)–N(1)	1.20(3)
Os(1)–Os(2)–Os(3)	58.65(4)	Os(1)–Os(3)–Os(2)	61.64(5)
Os(2)–Os(1)–Os(3)	59.70(5)	Os(1)–Os(2)–N(1)	68.4(7)
Os(2)–Os(1)–O(10)	68.1(5)	Os(2)–Os(1)–N(2)	109.8(7)
Os(1)–O(10)–N(1)	108(1)	Os(2)–N(1)–O(11)	133(2)
Os(2)–N(1)–O(10)	115(1)	O(10)–N(1)–O(11)	110(2)

oxygen atom of the nitrite moiety and incoming amino ligands. As the steric interaction of the R group on the amine is increased, the effect on the stereoselectivity of the substitution of CO groups will become more obvious and can be reflected by the yields of the products. Attempts to explain the distribution of the two isomers based on electronic effects experienced by the osmium metal centres are not very conclusive at this stage. In the case of phosphine-substituted derivatives, both isomers appeared to be formed in very similar yield. This is presumably due to a longer Os–P compared to Os–N bond which decreases the steric effect between the unsymmetrical NO_2 group and the ligand.

Hydrogenation of $[Os_3(\mu\text{-H})(CO)_9(\mu\text{-}\eta^2\text{-}NO_2)(NH_3)]$ **2a** in *n*-hexane at reflux afforded some insoluble solids which may be polymeric nitrite clusters. It is believed that both nitrosyl and nitrite clusters can be polymerised under thermal conditions. A similar observation has been reported by Norton *et al.*[17] in the reaction of $[N(PPh_3)_2][Ru_3(CO)_{10}(NO)]$ with gaseous nitric oxide.

Reaction of $[Os_3(\mu\text{-H})(CO)_{10}(\mu\text{-}\eta^2\text{-}NO_2)]$ 1 with 2-phenylethylamine

Reaction of cluster **1** with 2-phenylethylamine in refluxing $CHCl_3$ afforded two products. The major product was characterised as $[Os_3(\mu\text{-H})(CO)_9(\mu\text{-}\eta^2\text{-}NO_2)(NH_2CH_2CH_2Ph)]$ **3a** and the minor product is an isomer of cluster **3a** namely **3b**. Carbonylation of cluster **3a** or **3b** in $CHCl_3$ under thermal conditions afforded a yellow solid characterised as $[Os_3(\mu\text{-H})(CO)_{10}(\mu\text{-NHCH}_2CH_2Ph)]$ **4** (Scheme 1). The solid-state IR spectra (KBr disc) of clusters **3a** and **3b** show the $\nu(NO_2)$

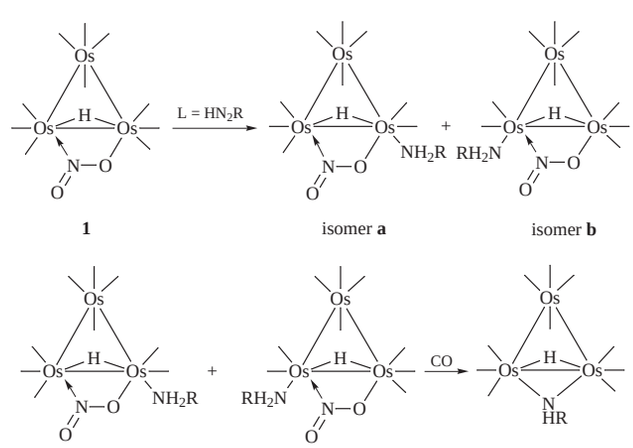

Scheme 1 R = H, **2a** (35%), **2b** (20%); R = CH_2CH_2Ph, **3a** (25%), **3b** (10%); R = $(CH_2)_{17}CH_3$, **5a** (20%), **5b** (5%); R = $C_6H_{10}Bu^t$-4, **6a** (20%), **6b** (<3%); L = pipea, **7a** (30%), **7b** (11%).

Table 3 Selected bond parameters (distances in Å, angles in °) of $[Os_3(\mu\text{-H})(CO)_{10}(\mu\text{-NHCH}_2CH_2Ph)]$ **4**

Os(1)–Os(2)	2.800(2)	Os(1)–Os(3)	2.853(2)
Os(2)–Os(3)	2.848(2)	Os(1)–N(1)	2.12(2)
Os(2)–N(1)	2.13(3)		
Os(1)–Os(2)–Os(3)	60.67(4)	Os(1)–Os(3)–Os(2)	58.82(5)
Os(2)–Os(1)–Os(3)	60.51(5)	Os(1)–N(1)–Os(2)	82.4(9)

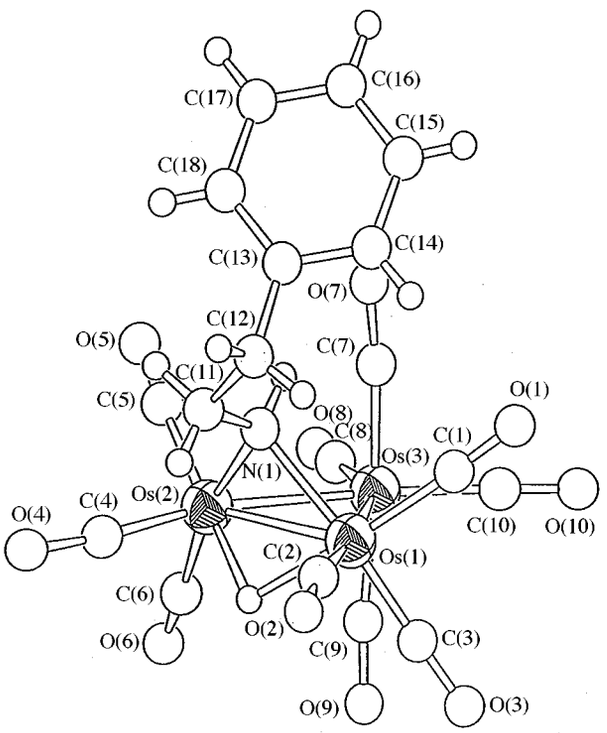

Fig. 2 Molecular structure of $[Os_3(\mu\text{-H})(CO)_{10}(\mu\text{-NHCH}_2CH_2Ph)]$ **4**.

stretching frequencies at 1484 and 1127 and 1480 and 1130 cm^{-1} respectively. No $\nu(NO_2)$ stretching was observed in the solid-state IR of cluster **4** which is consistent with loss of the nitrite ligand under thermal conditions. The ^1H NMR spectra of isomers **3a** and **3b** show bridging hydride signals at δ −11.4 and −11.5 respectively. In the spectrum of cluster **4** a bridging hydride at δ −14.8 and a broad singlet at δ 3.9 assigned to the μ-NH were also observed. The positive FAB mass spectra of clusters **3a** and **3b** show identical molecular peaks at *m*/*z* 991 that also supports the formulation of these isomers. The spectrum of cluster **4** exhibits a molecular ion peak at *m*/*z* 974 with daughter ions due to the sequential loss of ten carbonyls.

Yellow crystals of cluster **4** suitable for X-ray analysis were obtained by diffusion of layered *n*-hexane into a CH_2Cl_2 solution at room temperature. A perspective view of **4** is shown in Fig. 2 and selected bond parameters are given in Table 3. The Os(3) atom is co-ordinated to four carbonyls and the other two osmium atoms, Os(1) and Os(2), are bonded to three terminal carbonyls, a bridging hydride and a bridging amino ligand arranged *exo*. As the bridging nitrite is displaced by the amino ligand, the bridged edge Os(1)–Os(2) [2.800(2) Å] is now shorter than the other two Os–Os edges [Os(1)–Os(3) 2.853(2) and Os(2)–Os(3) 2.848(2) Å]. The bridged Os–Os edge in **4** is significantly shorter compared to that of cluster **1** [2.906(1) Å].

The elimination of the NO_2 group from cluster **3a** or **3b** is somewhat surprising and unprecedented in nitrite containing clusters. The mechanism is not clear, however in the absence of CO only a trace amount of cluster **4** can be obtained from thermolysis of isomers **3a** and **3b**. There have been numerous studies on the reduction of metal bound NO_2 to NO in systems such as $[M(CO)_x(NO_2)_y]$, M = Mn, Re, Cr, Mo or W, with the involvement of CO.[18,19] It has been suggested that the nitro or

Table 4 Selected bond parameters (distances in Å, angles in °) of $[Os_3(\mu\text{-H})(CO)_9(\mu\text{-}\eta^2\text{-NO}_2)\{NH_2(CH_2)_{17}CH_3\}]$ **5a**

Os(1)–Os(2)	2.905(3)	Os(1)–Os(3)	2.805(2)
Os(2)–Os(3)	2.857(2)	Os(1)–N(2)	2.29(3)
Os(1)–O(10)	2.17(2)	Os(2)–N(1)	2.05(3)
O(10)–N(1)	1.25(4)	O(11)–N(1)	1.26(3)
Os(1)–Os(2)–Os(3)	58.25(6)	Os(1)–Os(3)–Os(2)	61.71(6)
Os(2)–Os(1)–Os(3)	60.03(6)	Os(1)–Os(2)–N(1)	65.1(9)
Os(2)–Os(1)–O(10)	68.2(8)	Os(2)–Os(1)–N(2)	102.7(9)
Os(1)–O(10)–N(1)	104(2)	Os(2)–N(1)–O(10)	122(2)
Os(2)–N(1)–O(11)	126(2)	O(10)–N(1)–O(11)	110(3)

nitrite ligands on the metal complexes can be reduced to NO by oxygen-atom transfer from the NO_2^- moiety to a CO molecule.[20] A similar observation has also been reported in the reaction of $[Pd_3(O_2CMe)_5(\eta\text{-NO}_2)]$ with CO and HNO_2 to give the nitrosyl complexes, $[Pd_4(O_2CMe)_6(\mu\text{-NO})_2]$ and $[Pd_6(O_2CMe)_8(\mu\text{-NO})_2]$. Then the nitrosyl ligands were substituted by an excess of CO to give $[Pd_4(O_2CMe)_4(CO)_4]$ as the end product.[21] Johnson and co-workers[22] reported that the nitrosyl cluster $[Os_3(CO)_9(NO)_2]$ in the presence of CO afforded $[Os_3(CO)_{10}(NO)]^-$.

Reaction of $[Os_3(\mu\text{-H})(CO)_{10}(\mu\text{-}\eta^2\text{-NO}_2)]$ 1 with octadecylamine

Cluster **1** was treated with an excess of octadecylamine in CH_2Cl_2 to give two isomeric products which were characterised to be $[Os_3(\mu\text{-H})(CO)_9(\mu\text{-}\eta^2\text{-NO}_2)\{NH_2(CH_2)_{17}CH_3\}]$ **5a** and **5b**. The ^1H NMR spectra of clusters **5a** and **5b** exhibit a hydride resonance at δ −11.3 and −11.1 respectively. However, the NH signal is not observed even at low temperature (−50 °C). The positive FAB mass spectra showed identical molecular ion peaks. The molecular structure of cluster **5a** was revealed by X-ray analysis. A perspective view of **5a** is depicted in Fig. 3 and selected bond parameters are given in Table 4.

The $Os_3(NO_2)$ core is similar to that of cluster **1**. The hydride bridges across the longest Os(1)–Os(2) edge [2.905(3) Å]. The long alkylamino ligand is bonded to the metal core *via* the Os(1)–N(2) bond [2.29(3) Å]. The octadecyl chain adopts an extended, staggered conformation. The elongated shape of the molecule is interesting and the head-to-tail separation is approximately 23 Å. A similar cluster containing an extended organic chain has been observed in $[Os_3(\mu\text{-H})_2(CO)_9(\mu_3\text{-CNC}_5H_4CH{=}NC_6H_4OC_{16}H_{33})]$.[23] An interesting aspect of the structure is the molecular packing in the crystal. A packing diagram of **5a** viewed down the crystallographic *b* axis is shown in Fig. 4. The rod-like molecules stack with the aliphatic octadecyl chains pointing towards each other so that a layer of hydrocarbon is sandwiched by two layers of transition-metal cluster core. The molecules in the crystal packing are separated with normal van der Waals distances, no intermolecular hydrogen bonds being detected. This sort of arrangement is also similar to that observed in a tetradecylcobalt organometallic complex and is reminiscent of surfactant molecules.[24]

Reaction of $[Os_3(\mu\text{-H})(CO)_{10}(\mu\text{-}\eta^2\text{-NO}_2)]$ 1 with 4-*tert*-butylcyclohexylamine

Reaction of cluster **1** with an excess of 4-*tert*-butylcyclohexylamine afforded two orange products. The major product was characterised as $[Os_3(\mu\text{-H})(CO)_9(\mu\text{-}\eta^2\text{-NO}_2)(NH_2C_6H_{10}Bu^t\text{-}4)]$ **6a** in 20% yield and the minor isomer **6b** in trace amount.

However, carbonylation of clusters **5a**, **5b**, **6a** or **6b** does not lead to any amido complexes. This is probably due to the steric hindrance of the bulky substituents on the amine.

Reaction of $[Os_3(\mu\text{-H})(CO)_{10}(\mu\text{-}\eta^2\text{-NO}_2)]$ 1 with piperidine-1-ethanamine

Reaction of cluster **1** with an excess of piperidine-1-ethanamine (pipea) in CH_2Cl_2 at room temperature also afforded a pair of

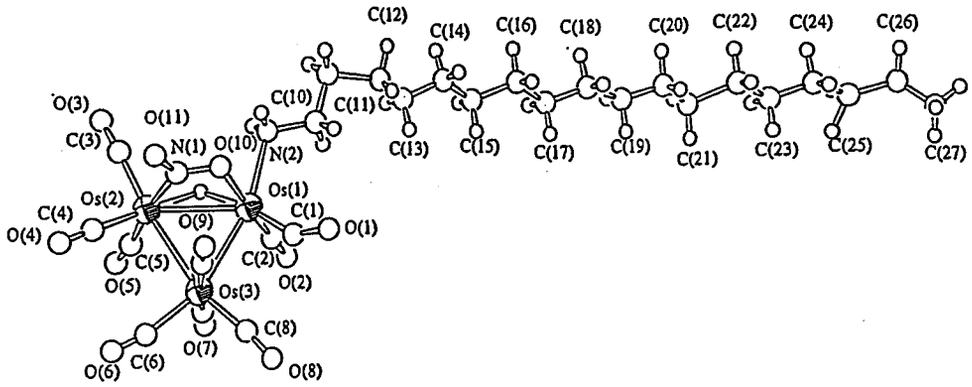

Fig. 3 Molecular structure of $[Os_3(\mu\text{-H})(CO)_9(\mu\text{-}\eta^2\text{-}NO_2)\{NH_2(CH_2)_{17}CH_3\}]$ **5a**.

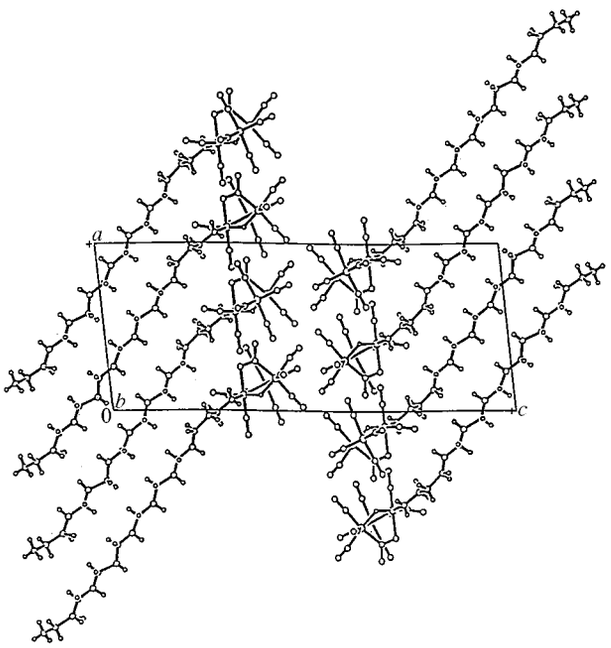

Fig. 4 Unit cell packing diagram of cluster **5a** (projection down the crystallographic *b* axis).

Table 5 Selected bond parameters (distances in Å, angles in °) of $[Os_3(\mu\text{-H})(CO)_9(\mu\text{-}\eta^2\text{-}NO_2)(pipea)]$ **7b**

Os(1)–Os(2)	2.859(1)	Os(1)–Os(3)	2.845(2)
Os(2)–Os(3)	2.851(1)	Os(2)–N(1)	2.10(2)
Os(3)–O(10)	2.16(1)	Os(2)–N(2)	2.20(2)
O(10)–N(1)	1.30(2)	O(11)–N(1)	1.23(2)
Os(1)–Os(2)–Os(3)	59.35(4)	Os(1)–Os(3)–Os(2)	61.10(3)
Os(2)–Os(1)–Os(3)	59.55(3)	Os(2)–Os(3)–O(10)	69.5(4)
Os(3)–Os(2)–N(1)	67.8(5)	Os(3)–Os(2)–N(2)	143.9(5)
Os(2)–N(1)–O(11)	129(1)	Os(2)–N(1)–O(10)	115(1)
Os(3)–O(10)–N(1)	106(1)	O(10)–N(1)–O(11)	114(1)

isomers **7a** and **7b** with formula $[Os_3(\mu\text{-H})(CO)_9(\mu\text{-}\eta^2\text{-}NO_2)$-(pipea)]. Carbonylation of either cluster **7a** or **7b** in $CHCl_3$ afforded $[Os_3(\mu\text{-H})(CO)_{10}(\mu\text{-pipea} - H)]$ **8** in 20% yield and $[Os_3(\mu\text{-H})(CO)_9(\mu\text{-}\eta^2\text{-pipea} - H)]$ **9** in a trace amount. However, thermolysis of **8** in $CHCl_3$ at reflux gave **9** in high yield. The molecular structures of clusters **7b**, **8** and **9** were established by X-ray crystallography. That of **7b** is depicted in Fig. 5 and selected bond parameters are given in Table 5. The molecular structures of clusters **8** and **9** are illustrated in Figs. 6 and 7 respectively and selected bond parameters are given in Tables 6 and 7 respectively.

The hydride and the nitrite ligands are bonded to the Os(2)–Os(3) edge [2.851(1) Å] in cluster **7b**. The functionalised amine

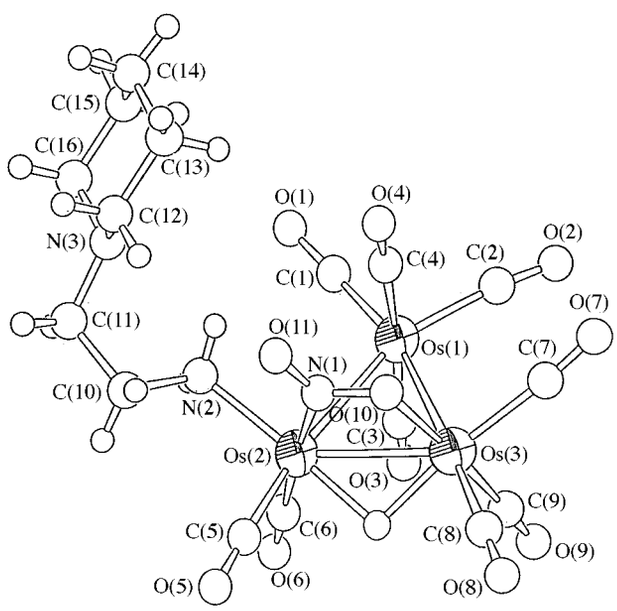

Fig. 5 Molecular structure of $[Os_3(\mu\text{-H})(CO)_9(\mu\text{-}\eta^2\text{-}NO_2)(pipea)]$ **7b**.

Table 6 Selected bond parameters (distances in Å, angles in °) of $[Os_3(\mu\text{-H})(CO)_{10}(\mu\text{-pipea} - H)]$ **8**

Os(1)–Os(2)	2.8038(8)	Os(1)–Os(3)	2.848(1)
Os(2)–Os(3)	2.8544(8)	Os(1)–N(1)	2.12(1)
Os(2)–N(2)	2.13(1)		
Os(1)–Os(2)–Os(3)	60.43(2)	Os(1)–Os(3)–Os(2)	58.91(2)
Os(2)–Os(1)–Os(3)	60.67(2)	Os(1)–N(1)–Os(2)	82.6(4)

is co-ordinated to the metal core *via* the primary amine in the equatorial position. In the reaction mixture, we have not isolated any complex with the tertiary amine substituted products in a significant amount. This observation is almost certainly due to the high nucleophilicity of the primary amine.

The three osmium atoms in cluster **8** defined an irregular triangle with Os(1)–Os(3) 2.848(1) and Os(2)–Os(3) 2.8544(8) Å being longer than the Os(1)–Os(2) bond [2.8038(8) Å]. The Os(3) atom is co-ordinated to four carbonyls and the other two osmium atoms, Os(1) and Os(2), to three terminal carbonyls, a bridging hydride and a bridging amino ligand. The bridging amino moiety is bonded to the metal core *via* N(1) in an *exo* arrangement similar to that observed in **4**.

In complex **9** the Os(3) atom is co-ordinated to four carbonyls and the other two osmium atoms, Os(1) and Os(2), to two and three terminal carbonyls respectively. The organic moiety is bonded to the core with a $\mu\text{-}\eta^2$ co-ordination mode. The amino moiety in the functionalised amine is bridged across the Os(1)–Os(2) edge *via* the Os–N bonds [Os(1)–N(1) 2.09(2) and Os(2)–

Table 7 Selected bond parameters (distances in Å, angles in °) of $[Os_3(\mu\text{-H})(CO)_9(\mu\text{-}\eta^2\text{-pipea} - H)]$ **9**

Os(1)–Os(2)	2.819(1)	Os(1)–Os(3)	2.814(1)
Os(2)–Os(3)	2.858(1)	Os(1)–N(1)	2.09(2)
Os(1)–N(2)	2.24(2)	Os(2)–N(1)	2.13(1)
N(1)–C(10)	1.51(3)	N(2)–C(11)	1.50(2)
C(10)–C(11)	1.54(3)		
Os(1)–Os(2)–Os(3)	59.43(3)	Os(1)–Os(3)–Os(2)	59.61(3)
Os(2)–Os(1)–Os(3)	60.96(3)	Os(1)–Os(2)–N(1)	47.5(4)
Os(2)–Os(1)–N(1)	100.8(4)	Os(1)–N(1)–Os(2)	83.9(6)
Os(1)–N(1)–C(10)	114(1)	Os(1)–N(2)–C(11)	104(1)
N(1)–C(10)–C(11)	106(1)	N(2)–C(11)–C(10)	114(1)

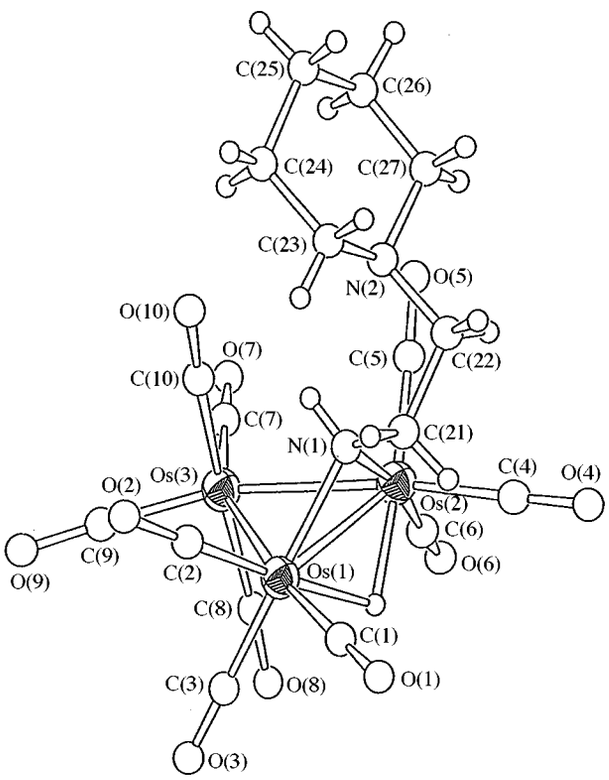

Fig. 6 Molecular structure of $[Os_3(\mu\text{-H})(CO)_{10}(\mu\text{-pipea} - H)]$ **8**.

N(1) 2.13(1) Å]. The piperidine nitrogen displaced one of the CO ligands in **8** to give a cyclometallated five-membered ring [Os(1), N(1), C(10), C(11), N(2)] so that two spiro ring systems with the common N(2) atom were formed.

Reaction of $[Os_3(\mu\text{-H})(CO)_{10}(\mu\text{-}\eta^2\text{-}NO_2)]$ 1 with 1-ethynylcyclohexylamine

Reaction of **1** with an excess of 1-ethynylcyclohexylamine (L) at room temperature afforded two orange isomeric products $[Os_3(\mu\text{-H})(CO)_9(\mu\text{-}\eta^2\text{-}NO_2)(echa)]$ **10a** and **10b**. Heating **10a** in $CHCl_3$ resulted in hydrogen migration, from the metal core to the unsaturated carbons, to give a pale orange complex $[Os_3(CO)_9(\mu\text{-}\eta^2\text{-}NO_2)(echa + H)]$ **11**, see Scheme 2. The bridged hydride on the metal core migrates to the terminal acetylene moiety with the formation of a metal–carbon bond. A similar hydride transfer to an organic fragment (phenylacetylene) has been observed in a triruthenium complex $[Ru_3(\mu\text{-H})_2(CO)_7(\mu_3\text{-L})(SiR_3)(PhC_2Ph)]$.[25]

The ^{1}H NMR spectra of clusters **10a** and **10b** exhibit a hydride resonance at δ −11.2 and −10.9 respectively. The signal due to the NH proton was observed at δ 5.6 and 5.3 respectively which indicated the functionalised amine co-ordinates to the electron-withdrawing $Os_3(NO_2)$ core. The acetylenic proton resonances were observed at δ 5.2 and 4.2 respectively. The ^{1}H NMR spectrum of **11** reveals no signal in the negative region

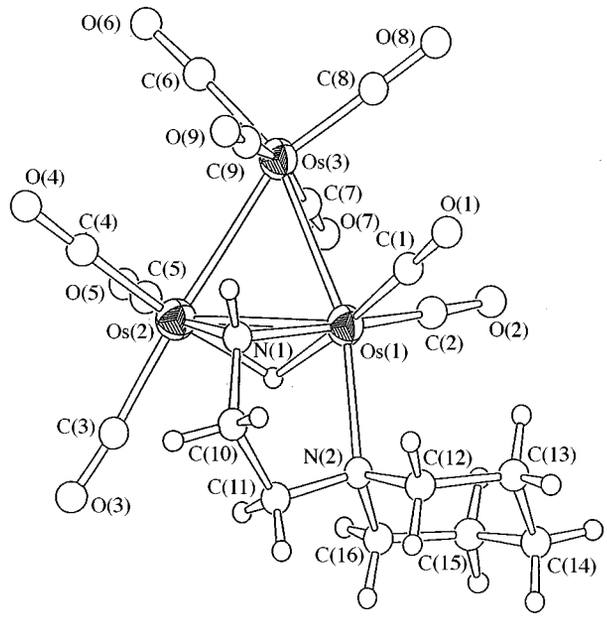

Fig. 7 Molecular structure of $[Os_3(\mu\text{-H})(CO)_9(\mu\text{-}\eta^2\text{-pipea} - H)]$ **9**.

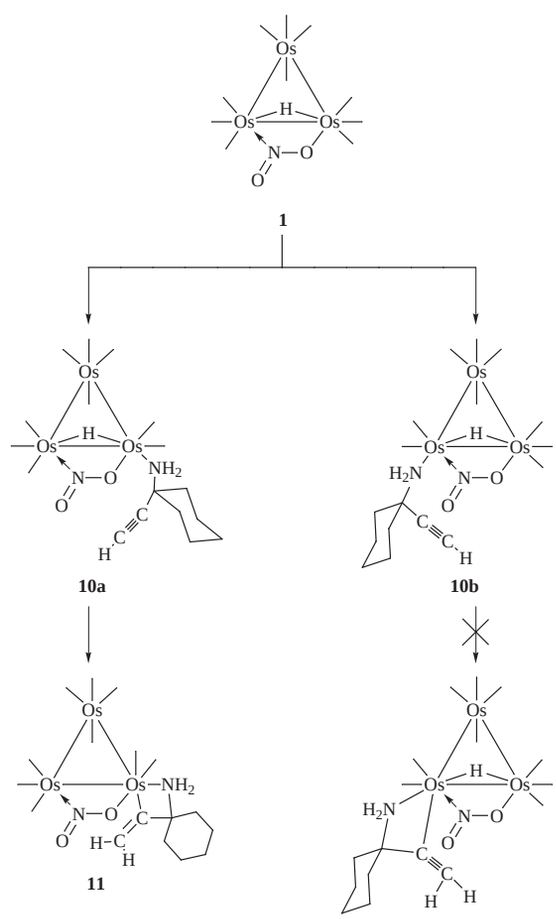

Scheme 2 Reaction of cluster **1** with 1-ethynylcyclohexylamine.

and a resonance appears at δ 5.4 with an integral corresponding to two hydrogen atoms. These spectroscopic data are consistent with the solid-state structure of **11** obtained by X-ray analysis. The molecular structure is shown in Fig. 8 and selected bond parameters are presented in Table 8.

The structure of cluster **11** consists of an $Os_3(NO_2)$ core similar to that of **2a**. Upon metal hydride migration to the unsaturated carbons in the functionalised amine, the 1-ethynylcyclohexylamine behaved as a bidentate chelate to Os(1) and led to the formation of a four-membered ring [Os(1), N(2), C(10),

Table 8 Selected bond parameters (distances in Å, angles in °) of $[Os_3(CO)_9(\mu\text{-}\eta^2\text{-}NO_2)(echa + H)]$ **11**

Os(2)–Os(3)	2.813(4)	Os(1)–Os(3)	2.896(4)
Os(1)–Os(2)	2.822(4)	Os(2)–N(1)	2.19(6)
Os(1)–N(2)	2.22(5)	Os(1)–O(10)	2.04(4)
Os(3)–C(16)	1.95(6)	O(10)–N(1)	1.37(7)
O(11)–N(1)	1.12(8)	C(10)–C(11)	1.50(9)
Os(2)–Os(1)–Os(3)	58.92(9)	Os(1)–Os(2)–Os(3)	61.8(5)
Os(1)–Os(3)–Os(2)	59.23(9)	Os(2)–Os(1)–O(10)	71(1)
Os(2)–Os(1)–N(2)	138(1)	Os(2)–N(1)–O(10)	109(4)
Os(2)–N(1)–O(11)	120(5)	Os(1)–N(2)–C(10)	88(3)
Os(1)–O(10)–N(1)	111(3)		

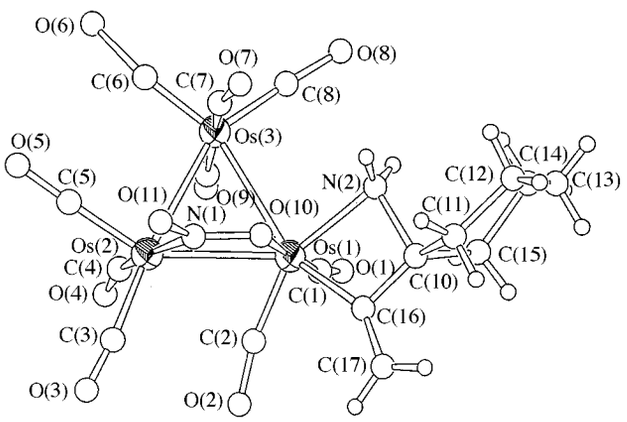

Fig. 8 Molecular structure of $[Os_3(CO)_9(\mu\text{-}\eta^2\text{-}NO_2)(echa + H)]$ **11**.

C(16)] with great angular strain. The Os(1)–Os(2) distance is significantly shorter than the corresponding Os–Os edge in **3a**.

It is noteworthy that only isomer **10a** will undergo hydrogen migration under thermal conditions; similar reaction has not been observed in **10b**. A steric repulsion between the organic moiety and the outstretched oxygen atom of the nitrite ligand will result in the corresponding rearranged product of **10b**.

Experimental

Although none of the compounds is particularly air or moisture sensitive, all the reactions were carried out under an inert atmosphere of argon using standard Schlenk techniques, unless otherwise indicated. Solvents used in all chemical reactions were of reagent grade, purified, and dried by distillation from the appropriate drying agents under nitrogen prior to use. Glassware was oven-dried at 130 °C. All chemicals, except where stated, were from commercial sources and used as supplied (Aldrich and Lancaster). Products were purified and separated by preparative thin-layer chromatography (TLC) on glass plates (20 × 20 cm) coated with Merck Kieselgel 60 GF_{254}.

Infrared spectra were recorded on a Bio-Rad FTS-7 IR or FTS-165 FT-IR spectrometer in CH_2Cl_2 using 0.5 mm CaF_2 solution cells with 0.5 mm path length or KBr pellets for the solid-state spectroscopy, ^1H NMR spectra on a Bruker DPX-300 NMR spectrometer and fast atom bombardment (FAB) mass spectra on a Finnigan MAT 95 mass spectrometer.

Reaction of $[Os_3(\mu\text{-}H)(CO)_{10}(\mu\text{-}\eta^2\text{-}NO_2)]$ 1 with NH_3

Complex **1** (50 mg, 0.055 mmol) with an excess of 2.0 M ammonia solution (in propan-2-ol) was stirred in 30 cm^3 CH_2Cl_2 at room temperature for 2 h. After removal of solvent under reduced pressure, the residue was separated by TLC on silica eluting with CH_2Cl_2–*n*-hexane (4:6 v/v) to give two products. The major orange band ($R_f \approx 0.3$) was characterised as $[Os_3(\mu\text{-}H)(CO)_9(\mu\text{-}\eta^2\text{-}NO_2)(NH_3)]$ **2a** (17 mg, 35%). Microcrystals were obtained by slow evaporation from a *n*-hexane solution over a period of 2 d (Found: C, 12.3; H, <0.5; N, 3.3. Calc.: C, 12.2; H, 0.5; N, 3.2%). The minor product **2b** ($R_f \approx 0.5$) was isomeric (9.7 mg, 20%) (Found: C, 12.4; H, <0.5; N, 3.2%).

Reaction of $[Os_3(\mu\text{-}H)(CO)_{10}(\mu\text{-}\eta^2\text{-}NO_2)]$ 1 with 2-phenylethylamine

Cluster **1** (50 mg, 0.055 mmol) was treated with an excess of 2-phenylethylamine in 30 cm^3 $CHCl_3$ at reflux for 20 h. The solution was concentrated under reduced pressure. Separation by TLC using CH_2Cl_2–*n*-hexane (4:6 v/v) as eluent afforded two products. The major product ($R_f \approx 0.45$) was characterised as $[Os_3(\mu\text{-}H)(CO)_9(\mu\text{-}\eta^2\text{-}NO_2)(NH_2CH_2CH_2Ph)]$ **3a** (13.6 mg, 25%). Microcrystals of **3a** were obtained by slow evaporation from a cyclohexane solution at −20 °C (Found: C, 20.6; H, 1.2; N, 2.8. Calc.: C, 20.6; H, 1.1; N, 3.0%). The minor band **3b** ($R_f \approx 0.55$) was characterised as an isomeric product (5.5 mg, 10%) (Found: C, 21.6; H, 1.1; N, 2.9%).

Carbonylation of clusters 3a and 3b

Cluster **3a** or **3b** (15 mg, 0.015 mmol) was dissolved in 20 cm^3 $CHCl_3$ with a continuous stream of CO bubbled through the orange solution. The solution was refluxed for 5 h to give a yellow solution. This solution was concentrated *in vacuo* and the residue chromatographed by TLC using CH_2Cl_2–*n*-hexane (1:1 v/v) as eluent to give an intense yellow band ($R_f \approx 0.45$). It was characterised as $[Os_3(\mu\text{-}H)(CO)_{10}(\mu\text{-}NHCH_2CH_2Ph)]$ **4** (6 mg, 41%). Yellow crystals were obtained by layered *n*-hexane diffusion into a CH_2Cl_2 solution.

Reaction of $[Os_3(\mu\text{-}H)(CO)_{10}(\mu\text{-}\eta^2\text{-}NO_2)]$ 1 with octadecylamine

Cluster **1** (50 mg, 0.055 mmol) was treated with an excess of octadecylamine in 30 cm^3 CH_2Cl_2 at room temperature for 30 h. The red solution was concentrated under reduced pressure and separated by TLC on silica. Elution with CH_2Cl_2–*n*-hexane (1:1 v/v) gave two bands. The major product ($R_f \approx 0.35$) was characterised as $[Os_3(\mu\text{-}H)(CO)_9(\mu\text{-}\eta^2\text{-}NO_2)\{NH_2(CH_2)_{17}CH_3\}]$ **5a**. Single crystals were obtained by slow evaporation from a CH_2Cl_2 solution (12.5 mg, 20%) (Found: C, 28.2; H, 3.4; N, 2.4. Calc.: C, 28.5; H, 3.5; N, 2.5%). The minor product **5b** ($R_f \approx 0.5$) was characterised as isomeric (3 mg, 5%).

Reaction of $[Os_3(\mu\text{-}H)(CO)_{10}(\mu\text{-}\eta^2\text{-}NO_2)]$ 1 with 4-*tert*-butylcyclohexylamine

Cluster **1** (50 mg, 0.055 mmol) was treated with an excess of 4-*tert*-butylcyclohexylamine in 30 cm^3 CH_2Cl_2 at 40 °C for 24 h. After removal of solvent under reduced pressure, TLC separation on silica eluted with CH_2Cl_2–*n*-hexane (1:1 v/v) to give a major orange product ($R_f \approx 0.55$). It was characterised as $[Os_3(\mu\text{-}H)(CO)_9(\mu\text{-}\eta^2\text{-}NO_2)(NH_2C_6H_{10}Bu^t\text{-}4)]$ **6a** (11.3 mg, 20%) (Found: C, 22.5; H, 2.0; N, 2.7. Calc.: C, 22.3; H, 2.2; N, 2.7%). The minor product **6b** ($R_f \approx 0.45$) was characterised as an isomer of **6a** (<3%).

Reaction of $[Os_3(\mu\text{-}H)(CO)_{10}(\mu\text{-}\eta^2\text{-}NO_2)]$ 1 with piperidine-1-ethanamine

Solid cluster **1** (100 mg, 0.11 mmol) was dissolved in 30 cm^3 CH_2Cl_2. The yellow solution was stirred with an excess of pipea at room temperature for 6 h, turning to orange. The solvent was removed *in vacuo*. The residue was separated by TLC using CH_2Cl_2–*n*-hexane (6:4 v/v) as eluent to give two bands. The top yellow band was unchanged **1** and the major yellow product ($R_f \approx 0.5$) was characterised as $[Os_3(\mu\text{-}H)(CO)_9(\mu\text{-}\eta^2\text{-}NO_2)$-(pipea)] **7a** (33 mg, 30%). The minor yellow product **7b** ($R_f \approx 0.35$) was characterised as an isomer of **7a** (12 mg, 11%). Yellow microcrystals were obtained from a *n*-hexane solution by slow evaporation (Found: C, 19.2; H, 1.9; N, 4.3. Calc.: C, 19.3; H, 1.7; N, 4.2%).

Table 9 Summary of crystal data, details of data collection, solution and refinement parameters for compounds **2a**–**11**

	2a	**4**	**5a**	**7b**	**8**	**9**	**11**
Empirical formula	$C_9H_4N_2O_{11}Os_3$	$C_{18}H_{11}NO_{10}Os_3$	$C_{27}H_{40}N_2O_{11}Os_3$	$C_{16}H_{17}N_3O_{11}Os_3$	$C_{17}H_{16}N_2O_{10}Os_3$	$C_{16}H_{16}N_2O_9Os_3$	$C_{17}H_{14}N_2O_{11}Os_3$
Formula weight	866.74	971.89	1139.22	997.92	978.92	950.91	992.90
Crystal colour, habit	Orange, block	Yellow, prism	Yellow, block	Orange, plate	Yellow, block	Yellow, plate	Orange, rod
Crystal size/mm	0.13 × 0.18 × 0.23	0.21 × 0.26 × 0.33	0.12 × 0.18 × 0.20	0.09 × 0.28 × 0.31	0.22 × 0.23 × 0.24	0.03 × 0.20 × 0.24	0.02 × 0.02 × 0.03
Crystal system	Monoclinic	Monoclinic	Monoclinic	Orthorhombic	Triclinic	Triclinic	Triclinic
Space group	$P2_1/c$ (no. 14)	$P2_1/n$ (no. 14)	$P2_1/a$ (no. 14)	*Pbca* (no. 61)	$P\bar{1}$ (no. 2)	$P\bar{1}$ (no. 2)	$P\bar{1}$ (no. 2)
a/Å	9.303(4)	11.139(4)	12.258(1)	22.172(6)	11.349(1)	8.496(1)	7.880(1)
b/Å	9.610(6)	14.604(4)	9.663(1)	17.821(3)	14.498(2)	10.301(1)	9.299(1)
c/Å	19.036(6)	14.069(4)	30.978(1)	12.552(4)	14.937(2)	13.527(2)	16.999(1)
α/°					101.87(1)	104.71(1)	95.64(2)
β/°	90.37(4)	95.77(3)	96.44(2)		90.84(1)	96.69(2)	91.36(2)
γ/°					93.29(2)	103.25(1)	112.58(2)
U/Å^3	1701(1)	2277(1)	3646.2(5)	4959(1)	2400.3(5)	1095.2(3)	1142.0(3)
Z	4	4	4	8	4	2	2
Temperature/K	298	298	298	298	298	298	298
D_c/g cm^{-3}	3.461	2.835	2.075	2.673	2.709	2.883	2.887
F(000)	1552	1736	2128	3600	1760	852	892
μ(Mo-Kα)/cm^{-1}	223.88	167.41	104.74	153.82	158.83	173.97	166.98
Reflections collected	2558	3307	24215	3881	39421	16668	10244
Unique reflections	2386	3124	3245	3667	8532	3478	2492
Observed reflections [$I > 3\sigma(I)$]	1452	2186	1729	1818	5688	2103	1233
R	0.046	0.062	0.067	0.040	0.047	0.043	0.098
R′	0.054	0.091	0.059	0.040	0.057	0.053	0.114
Goodness of fit	2.02	2.90	1.54	1.51	1.40	0.96	2.40

Carbonylation of $[Os_3(\mu\text{-H})(CO)_9(\mu\text{-}\eta^2\text{-}NO_2)(pipea)]$ 7a and 7b

Cluster **7a** or **7b** (30 mg, 0.03 mmol) was dissolved in 30 cm^3 $CHCl_3$ with a stream of CO bubbled through the solution. It was refluxed for 6 h to give a yellow solution. After the mixture was cooled to room temperature, the solvent was removed *in vacuo*. The residue was separated by TLC using CH_2Cl_2–*n*-hexane (1:1 v/v) as eluent to afford two yellow bands. The major yellow product ($R_f \approx 0.4$) was characterised as $[Os_3(\mu\text{-H})(CO)_{10}(\mu\text{-pipea} - H)]$ **8** (6 mg, 20%). Yellow microcrystals were obtained from a $CHCl_3$ solution by slow evaporation at −20 °C over a period of 2 d. The minor product ($R_f \approx 0.6$) was characterised as $[Os_3(\mu\text{-H})(CO)_9(\mu\text{-}\eta^2\text{-pipea} - H)]$ **9** in trace amount.

Improved synthesis of $[Os_3(\mu\text{-H})(CO)_9(\mu\text{-}\eta^2\text{-}NO_2)(\mu\text{-}\eta^2\text{-pipea} - H)]$ 9

Cluster **8** (30 mg, 0.03 mmol) was dissolved in 30 cm^3 $CHCl_3$ then refluxed for 18 h. The solution was cooled to room temperature. After removal of solvent, separation of the residue by TLC using CH_2Cl_2–*n*-hexane (1:1 v/v) as eluent afforded $[Os_3(\mu\text{-H})(CO)_9(\mu\text{-}\eta^2\text{-pipea} - H)]$ **9** in good yield (14 mg, 49%). Yellow crystals were obtained from a $CHCl_3$–cyclohexane solution by slow evaporation.

Reaction of $[Os_3(\mu\text{-H})(CO)_{10}(\mu\text{-}\eta^2\text{-}NO_2)]$ 1 with 1-ethynylcyclohexylamine

Cluster **1** (50 mg, 0.055 mmol) was treated with 1-ethynylcyclohexylamine (L) in 30 cm^3 $CHCl_3$ for 4 h. The solvent was removed *in vacuo*. Separation by TLC on silica, using CH_2Cl_2–*n*-hexane (1:1 v/v) as eluent, afforded two orange products. The major product ($R_f \approx 0.5$) was characterised as $[Os_3(\mu\text{-H})(CO)_9(\mu\text{-}\eta^2\text{-}NO_2)(echa)]$ **10a** (16 mg, 29%) (Found: C, 20.6; H, 1.5; N, 2.9. Calc.: C, 20.6; H, 1.4; N, 2.8%). The minor product **10b** ($R_f \approx 0.4$) was found to be isomeric and recrystallised from a $CHCl_3$ solution to give orange crystals (9 mg, 16%).

Thermolysis of $[Os_3(\mu\text{-H})(CO)_9(\mu\text{-}\eta^2\text{-}NO_2)(echa)]$ 10a

Cluster **10a** (20 mg, 0.020 mmol) was dissolved in 30 cm^3 $CHCl_3$ solution and stirred at reflux temperature for 8 h. After the mixture was cooled to room temperature, the solvent was removed *in vacuo*. The residue was subjected to TLC on silica using CH_2Cl_2–*n*-hexane (3:7 v/v) as eluent to give one intense yellow band ($R_f \approx 0.35$). It was characterised as cluster $[Os_3(CO)_9(\mu\text{-}\eta^2\text{-}NO_2)(echa + H)]$ **11** (10 mg, 50%) (Found: C, 20.7; H, 1.7; N, 2.9. Calc.: C, 20.6; H, 1.4; N, 2.8%). Microcrystals were obtained from a THF–*n*-hexane solution by slow evaporation over a period of 24 h.

X-Ray crystallography

All pertinent crystallographic data and other experimental details are summarised in Table 9. Intensity data were collected on either of the following diffractometers [Enraf-Nonius CAD4 diffractometer (**7b**), Rigaku AFC7R diffractometer (**2a** and **4**) and MAR Research Image Plate Scanner (**5a**, **8**, **9** and **11**)] with graphite-monochromated Mo-Kα radiation ($\lambda = 0.71073$ Å). For the Enraf-Nonius CAD4 and Rigaku AFC7R diffractometers, all data were collected using the ω–2θ scan technique, with selected scan rates, ranges and widths depending on the crystal size, shape, mosaicity and divergence of the primary X-ray beam. For the image plate scanner, data were collected using $3 \times 65°$ frames with an exposure time of 5 min per frame. All data sets were collected for Lorentz-polarisation effects and absorption collections based on ψ-scan methods[26] were also applied for clusters **2a**, **4** and **7b**. An approximate absorption correction was made by inter-image scaling for the structures of **5a**, **8**, **9** and **11**.

The space groups of the crystals were determined from the systematic absences of the reflections. In cases where the space group could not be determined unambiguously, structure solution followed by refinement for all possible alternatives were undertaken and then the results were compared. All structures were solved by a combination of direct methods (SIR 88,[27] SIR 92[28] and DIRDIF 94[29]) and Fourier-difference techniques. Refinements were carried out by full-matrix least-squares analysis on *F* with all metal atoms and other non-hydrogen atoms refined anisotropically, until convergence was reached ($\Delta/\sigma < 0.1$). Hydrogen atoms on the organic ligands were generated in their idealised positions (C–H 0.95 Å) unless otherwise specified while the metal hydrides were estimated by potential energy calculations.[30] All hydrogen atoms were included in the structure factor calculations but the parameters were fixed without further refinement. All calculations were performed on a Silicon-Graphics computer using the program package TEXSAN.[31]

CCDC reference number 186/1203.

Acknowledgements

We thank the Hong Kong Research Grants Council and the University of Hong Kong for financial support. B. K.-M. Hui acknowledges the receipt of a postgraduate studentship, administered by the University of Hong Kong.

References

1 C. C. Yin and A. J. Deeming, *J. Chem. Soc.*, *Dalton Trans.*, 1975, 2091.
2 B. F. G. Johnson, J. Lewis and D. A. Pippard, *J. Chem. Soc.*, *Dalton Trans.*, 1981, 407.
3 B. F. G. Johnson, J. Lewis, T. I. Odiaka and P. R. Raithby, *J. Organomet. Chem.*, 1981, **216**, C56.
4 K. Burgess, B. F. G. Johnson and J. Lewis, *J. Organomet. Chem.*, 1982, **233**, C55.
5 A. Eisenstadt, C. M. Giandomenico, M. F. Frederick and R. M. Laine, *Organometallics*, 1985, **4**, 2033.
6 R. H. Fish, T. Kim, J. L. Stewart, J. H. Bushweller, R. K. Rosen and J. W. Dupon, *Organometallics*, 1986, **5**, 2193.
7 J. R. Sharpley, D. E. Samkoff, C. Bueno and M. R. Churchill, *Inorg. Chem.*, 1982, **21**, 634.
8 M. R. Churchill and J. R. Missert, *J. Organomet. Chem.*, 1983, **256**, 349.
9 K. A. Azam, A. J. Deeming, I. P. Rothwell, M. B. Hursthouse and J. D. J. Backer-Dirks, *J. Chem. Soc.*, *Dalton Trans.*, 1981, 2039.
10 A. J. Deeming, R. Peters, M. B. Hursthouse and J. D. J. Backer-Dirks, *J. Chem. Soc.*, *Dalton Trans.*, 1982, 787.
11 A. J. Deeming, R. Peters, M. B. Hursthouse and J. D. J. Backer-Dirks, *J. Chem. Soc.*, *Dalton Trans.*, 1982, 1205.
12 G. A. Foulds, B. F. G. Johnson and J. Lewis, *J. Organomet. Chem.*, 1985, **296**, 147.
13 B. K. M. Hui and W. T. Wong, *J. Chem. Soc.*, *Dalton Trans.*, 1996, 2177.
14 B. K. M. Hui and W. T. Wong, *J. Chem. Soc.*, *Dalton Trans.*, 1998, 447.
15 A. J. Finney, M. A. Hitchman, C. L. Raston, G. L. Rowbottom, B. W. Skelton and A. H. White, *Aust. J. Chem.*, 1981, **34**, 2113.
16 A. J. Finney, M. A. Hitchman, C. L. Raston, G. L. Rowbottom, B. W. Skelton and A. H. White, *Aust. J. Chem.*, 1981, **34**, 2905.
17 J. R. Norton, J. P. Collman, G. Dolcetti and W. T. Robinson, *Inorg. Chem.*, 1972, **11**, 382.
18 B. F. G. Johnson, A. Sieker, A. J. Blake and R. E. P. Winpenny, *J. Chem. Soc.*, *Chem. Commun.*, 1993, 1345.
19 A. Sieker, A. J. Blake, S. Parsons and B. F. G. Johnson, *J. Chem. Soc.*, *Dalton Trans.*, 1995, 1391.
20 A. Sieker, A. J. Blake and B. F. G. Johnson, *J. Chem. Soc.*, *Dalton Trans.*, 1996, 1419.
21 A. Chiesa, R. Ugo, A. Sironi and A. Yatsimirski, *J. Chem. Soc.*, *Chem. Commun.*, 1990, 350.
22 S. Bhaduri, B. F. G. Johnson, J. Lewis, D. J. Watson and C. Zuccaro, *J. Chem. Soc.*, *Dalton Trans.*, 1979, 557.
23 W. Y. Wong, S. Chan and W. T. Wong, *J. Chem. Soc.*, *Dalton Trans.*, 1996, 2293.
24 E. J. Starr, S. A. Bourne, M. R. Caiva and J. R. Moss, *J. Organomet. Chem.*, 1995, **490**, C20.
25 J. A. Cabeza, S. Garcia-Granda, A. Llamazares, V. Riera and J. F. Van der Maelen, *Organometallics*, 1993, **12**, 2973; J. A. Cabeza,

I. Del Rio M. Moreno and V. Riera, *Organometallics*, 1998, **17**, 3027.
26 A. C. T. North, D. C. Philips and F. S. Mathews, *Acta Crystallogr., Sect. A*, 1968, **24**, 351.
27 M. C. Burla, M. Camalli, G. Cascarano, C. Giacovazzo, G. Polidori, R. Spagna and D. Viterbo, *J. Appl. Crystallogr.*, 1989, **22**, 389.
28 A. Altomare, M. C. Burla, M. Camalli, G. Cascarano, C. Giacovazzo, A. Guagliardi and G. Polidori, *J. Appl. Crystallogr.*, 1994, **27**, 435.
29 P. T. Beurskens, G. Admiraals, G. Beurskens, W. P. Bosman, R. de Gelder, R. Israel and J. M. M. Smits, The DIRDIF 94 program system, Technical Report of the Crystallography Laboratory, the University of Nijmegen, 1994.
30 A. G. Orpen, *J. Chem. Soc., Dalton Trans.*, 1980, 2509.
31 TEXSAN, Crystal Structure Analysis Package, Molecular Structure Corporation, Houston, TX, 1985 and 1992.

Paper 8/05241G